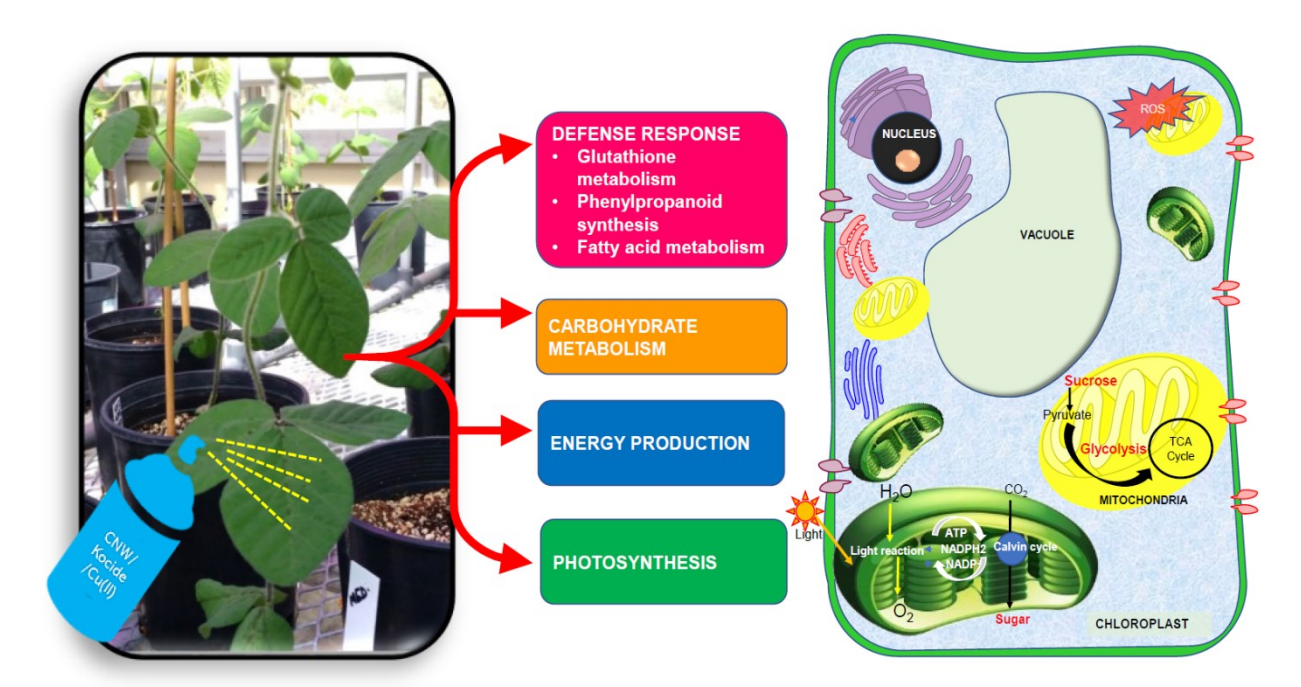
1	Unraveling metabolic and proteomic features in soybean plants in response to copper
2	hydroxide nanowires compared to a commercial fertilizer
3 4 5 6 7 8	Sanghamitra Majumdar, <sup>1,2</sup> Randall Long, <sup>3</sup> Jay Kirkwood, <sup>4</sup> Anastasiia S. Minakova, <sup>1</sup> Arturo A. Keller, <sup>1,2</sup> *
9 10	<sup>1</sup> Bren School of Environmental Science and Management, University of California, Santa
11	Barbara, California 93106, United States
12	<sup>2</sup> University of California, Center for Environmental Implications of Nanotechnology, Santa
13	Barbara, California 93106, United States
14	<sup>3</sup> Ecology, Evolution, and Marine Biology, University of California, Santa Barbara, California
15	93106, United States
16	<sup>4</sup> Institute for Integrative Genome Biology, Department of Botany and Plant Sciences, University
17	of California, Riverside, California 92521, United States
18 19 20 21 22 23 24 25 26 27 28 29 31 32 33	*Corresponding author Dr. Arturo A. Keller Professor, School of Environmental Science and Management 3420 Bren Hall University of California Santa Barbara, CA 93106 Tel. 805-893-7548
35 36	Fax: 805-893-7612 Email: keller@bren.ucsb.edu

## 37 TOC Graphic



#### Abstract

Mechanistic understanding of the interaction of copper-based nanomaterials with crops is crucial for exploring their application in precision agriculture and their implications on plant health. We investigated the biological response of soybean (*Glycine max*) plants to foliar application of copper hydroxide nanowires (CNW) at realistic exposure concentrations. Commercial copper hydroxide-containing fungicide (Kocide), copper ions, and untreated controls were used for comparison to identify unique features at physiological, cellular, and molecular levels. After 32-d exposure to CNW (0.36, 1.8, and 9 mg CNW/plant), newly developed tissues accumulated significantly high levels of Cu (18-60  $\mu$ g/g), compared to Kocide (10  $\mu$ g/g); however the rate of Cu translocation from site of CNW treatment to other tissues was slower compared to other Cu treatments. CNW treatments altered Co, Mn, Zn, and Fe accumulation in the tissues, and enhanced photosynthetic activities at medium and high exposure dose, similar to Kocide treatment. Proteomics and metabolomic analysis of leaves from soybean plants exposed to CNW treatments

suggests dose-dependent response, resulting in the activation of major biological processes, including photosynthesis, energy production, fatty acid metabolism, lignin biosynthesis, and carbohydrate metabolism. In contrast to CNW treatments, Kocide exposure resulted in increased oxidative stress response and amino acid metabolism activation.

**Keywords:** copper hydroxide nanowires, Kocide, soybean, proteomics, metabolomics, gas exchange, lignin

#### **SYNOPSIS**

Soybean plants exposed to copper hydroxide nanowires differentially accumulated proteins and metabolites related to photosynthetic process, energy production, carbohydrate metabolism, and fatty acid metabolism.

72

73

74

75

76

77

78

79

80

81

82

83

84

85

86

87

88

89

90

68

69

70

71

#### INTRODUCTION

Nanotechnology has evidently become a promising tool in precision agriculture that provides opportunities to utilize resources in a more efficient and strategic manner with reduced environmental impact and costs.1 There is a steady increase in the development of novel agrochemical products employing nanomaterials by adapting traditional ones to enhance their effectiveness, absorption and controlled release to regions of interest in crops. However, this also brings significant regulatory challenges due to limited understanding of their mechanism of action, and long-term impact on the environment and human health. The U.S. Environmental Protection Agency regulates the use of nanomaterials in pesticide products under the Federal Insecticide, Fungicide, and Rodenticide Act (FIFRA), and is responsible for determining their efficacy, safety, and conditions that can limit or eliminate any potential risks.<sup>2</sup> However, there is a substantial need to adopt modern hazard evaluation and risk-assessment protocols and utilize high-throughput methods to determine the mechanism of action of novel nanomaterials, understand their benefits and potential unintended effects.<sup>3</sup> Copper is an essential nutrient that is critical to plant metabolic processes including photosynthesis, electron transport, respiration, oxidative stress response, hormone signaling, cell wall metabolism, transcription signaling, protein trafficking, oxidative phosphorylation and iron mobilization.<sup>4</sup> It also acts as a cofactor in metalloproteins such as cytochrome-c oxidase in

mitochondria, plastocyanin and polyphenol oxidase in chloroplast, extracellular laccases, and Cu/Zn superoxide dismutase (SOD) in cytosol and chloroplast. However, at high concentrations, redox cycling between Cu oxidation states can catalyze the production of hydroxyl radicals which can damage biomolecules. 6 Copper is used in numerous registered agrochemicals, in the form of copper sulfate pentahydrate, basic copper sulfate, copper hydroxide, cuprous oxide, copper oxychloride, copper ammonium carbonate, and copper octanoate. The ability of Cu ions to bind to functional groups of proteins to cause protein denaturation and cell damage is leveraged in crop protection. Some commercial pesticides such as CuPro and Kocide®-3000 DuPont<sup>TM</sup> (Kocide) are constituted of Cu(OH)<sub>2</sub> nanosheets; however, given the micron-scale size of the final material, these pesticides are not regulated as "nanopesticides".8 The effects of nanoscale-Cu-based formulations have been shown to vary across crop species depending on the particle properties, mode of application and growth conditions. 9-16 Metabolomic studies in lettuce, cucumber, corn and maize show implications for energy metabolism and plant defense system. 11, 17, 18 Recent studies show that CuO nanoparticles (nCuO), Cu<sub>3</sub>(PO<sub>4</sub>)<sub>2</sub> nanosheets and CuO nanosheets enhance nutrient acquisition and bolster plant's innate defense system by transcription of defense and health related genes. 19-21 Although the effects of Kocide has been studied widely in crops at physiological and metabolic level, the underlying mechanisms at the protein level are unexplored. In addition, there is limited information on the interaction of crops with nanoscale-Cu(OH)<sub>2</sub> particles which show potential agronomic benefits comparable to Kocide. 22 Soybean (Glycine max) is a globally important legume crop which is a major source of proteins and fatty acids, and a good candidate to study discovery proteomics and metabolomics due to incrementing data availability on the functional annotation of soybean genes.<sup>23</sup>

91

92

93

94

95

96

97

98

99

100

101

102

103

104

105

106

107

108

109

110

111

The current study evaluates the hypotheses that soybean plants will demonstrate increased photosynthetic potential in response to Cu(OH)<sub>2</sub> nanowires (CNW) compared to untreated controls, and the underlying mechanism aided by the responsive proteins and metabolites will be distinct from Kocide and dissolved Cu(II)-ion exposures. We investigate the effect of foliar application of CNWs at realistic exposure concentrations on nutrient accumulation, lignification, and photosynthesis in soybean plants during vegetative and flowering stages under greenhouse conditions. These endpoints were compared with untreated controls, micron-sized Kocide and dissolved Cu(II)-ion exposures. Liquid chromatography-tandem mass spectrometry (LC-MS/MS) based proteomic and metabolomic analyses of leaves were used to identify the biomarkers of exposure unique to CNWs treatments.

#### MATERIALS AND METHODS

#### Chemicals

CNW (50 nm dia., 3-5 μm long, 99.5% pure, 65% Cu) were procured from US Research Nanomaterials Inc. As per manufacturer's report, these particles are produced by calcination and precipitation without addition of any stabilizer. For a comparative exposure assessment, we used a commercial Cu(OH)<sub>2</sub>-based fungicide product, Kocide®-3000 DuPont<sup>TM</sup> (26.5% Cu) and CuSO<sub>4</sub>.5H<sub>2</sub>O (25.4% Cu, referred as CuSO<sub>4</sub>).

#### **Plant Growth Conditions**

Soybean (*Glycine max* L. var. Envy) seeds purchased from Seed Savers Exchange (Decorah, Iowa, USA) were surface sterilized with 2% sodium hypochlorite solution, rinsed thoroughly and soaked in nanopure water (NPW,  $18.2M\Omega$ .cm at  $25^{\circ}$ C) for 1 h. The seeds were germinated in seed-starter trays and then grown in small pots (10.2 cm x 7.6 cm; three seedlings/pot) for 22 days. Upon the appearance of the first true leaf, each healthy and uniform-

sized seedling was transplanted to individual pots (20.5 cm. x 21.6 cm) and used for exposure assay after 2 days. Artificial soil mixture composed of sand (Quikrete Washed Plaster Sand), organic potting-mix, vermiculite (Therm-O-Rock), coco coir (Canna), and perlite (Therm-O-Rock), at a ratio of 1:1:2:3:4 by volume was used for germination and plant growth. The soil mixture was amended with 0.4% (v/v) 4-4-4 NPK-fertilizer. Plants were grown in greenhouse conditions, maintained at 25 ± 3 °C and 14 h photoperiod throughout the experiment. Plants were irrigated every alternate day with NPW.

### **Foliar Spray Exposure Experiment**

136

137

138

139

140

141

142

143

144

145

146

147

148

149

150

151

152

153

154

155

156

157

158

For foliar exposure, 24-d-old soybean plants were sprayed with aqueous colloidal suspensions of CNW or Kocide, or CuSO<sub>4</sub> solution, or NPW, using a commercial hand-held sprayer. The doses were selected based on manufacturer's recommendation for field application of Kocide on soybean plants (0.84 - 1.68 kg/ha  $\approx 2.2$  - 4.5 mg/plant). The higher application rate was selected for the exposure studies, which represents 1.2 mg Cu/plant. Three different treatment levels were selected for CNW, (CNW-L: 0.36, CNW-M: 1.8, and CNW-H: 9 mg CNW/plant, contributing 0.24, 1.2, and 6 mg Cu/plant, respectively). Preliminary dissolution studies using Amicon 3KDa centrifugal filters suggested ≤ 10% dissolution of Cu(II)-ions from CNW suspensions. Thus, to evaluate the effect of dissolved Cu(II)-ions, CuSO<sub>4</sub> exposure with a dose equivalent to 10% CNW-M was chosen (0.48 mg CuSO<sub>4</sub>/plant). Foliar spray was optimized for delivering and reporting accurate exposure doses. Preliminary experiments suggested that only 10% of a spray volume from the hand-held sprayer is retained by the soybean foliage (~0.001 L). To supply the requisite amount of Cu from the different treatments in a total volume of 6 ml, 80 mg/L CuSO<sub>4</sub>, 755 mg/L Kocide, and 60, 300 and 1500 mg/L CNW treatments were prepared fresh on the day of exposure. CNW and Kocide treatments were prepared by sonicating 0.05 L of each suspension for 5 min using a sonication probe fitted with a microtip (S-4000, Misonix Ultrasonic, USA) at 40% amplitude (input power 7 W) (Supporting Information, SI-Figure S1). To avoid overheating, pulsed sonication for 2 s was adopted and the tubes were kept in a secondary container with ice water. The suspensions were diluted 4 times with NPW, followed by a 15 min bath sonication (Branson 8800, Danbury, CT, USA). The average hydrodynamic diameter and zeta ( $\zeta$ )-potential of the suspended CNW and Kocide particles were measured immediately after bath sonication using a Zetasizer Nano-ZS (Malvern Instruments, Worcestershire, UK) at 25°C. The stability of the suspensions was tested after 0, 24, 48, and 96 h of preparation. Plants were sprayed in six separate spray events over two days, under shade without any direct artificial or natural lighting. Each day the plants were sprayed three times, with a 1 h interval between each event to allow the droplets to dry. The plants were weighed before and after each spraying event to report the exact dose. The average cumulative mass of the suspensions retained on the aerial tissues after six spray events across all the treatments was recorded as  $6.1 \pm 0.1$  g. The soil was covered with a customized plastic cover to avoid contamination from the spray or dripping of excess droplets from the leaves (SI-Figure S1). The experiment was conducted in two staggered sets, each used for different experimental goals. Each set consisted of four replicates per treatment, including an "untreated control" where NPW was sprayed to the foliage. The pots were randomly arranged on the greenhouse bench and rearranged twice a week.

### **Physiological Parameters and Element Content**

159

160

161

162

163

164

165

166

167

168

169

170

171

172

173

174

175

176

177

178

179

180

181

The first set of soybean plants was used to record physiological and gas exchange parameters periodically, and the plants were harvested after 16- and 32-d of exposure to determine elemental content in the tissues. The roots were washed under tap water to discard the adhered soil

particles, followed by rinsing the plant three times alternately with 0.1% (v/v) HNO<sub>3</sub> and NPW. To test the extent of adsorption and absorption of various treatments on the aerial tissues, two separate sets of three plants were analyzed for total Cu content after 1-d of exposure, with and without rinsing the shoots. Shoot and root lengths were measured to evaluate the effects on plant growth and overt plant health in response to different Cu treatments. The wet plants were dried at 25°C for 1 h, roots and stems were separated, and fresh biomass was recorded across all the treatments. Roots and shoots were dried at 70°C for 96 h, weighed, and digested using 1:4 (v/v) HNO<sub>3</sub>:H<sub>2</sub>O<sub>2</sub> heated at 115°C for 40 min on a heat block (DigiPREP System; SCP Science). The digested contents were diluted to fit the calibration curve prepared using multi-elemental standards. A standard reference material (Spinach leaves, NIST 1570A) was processed with every batch of samples, and ≥95% recovery was achieved for all the elements. The digested tissues were analyzed for Cu, macro-nutrients (Ca, K, Mg, Na, P), and micro-nutrients (Co, Fe, Mn, Mo, Ni, Zn) using ICP-MS (Agilent ICP-MS 7500, Agilent Technologies, Santa Clara, CA, USA). Analytical and matrix blanks were analyzed, and a calibration verification standard was run every 12 samples.

### **Gas Exchange Measurements**

182

183

184

185

186

187

188

189

190

191

192

193

194

195

196

197

198

199

200

201

202

203

204

Spot gas exchange surveys were performed on 5-, 12- and 21-d after foliar exposure, using a portable infrared gas analyzer (LI-6400xt, LI-COR, Lincoln, NE, USA) equipped with a 2×3 cm² leaf chamber and a red/blue light-source (6400-02B, LI-COR), as described in details in SI Method S1. Briefly, the measurements were made by selecting the most recent fully expanded leaf, typically the second or third one from the apical meristem and allowing the leaf to adapt to the chamber for approximately 2 min. Three measurements were averaged to obtain net photosynthesis (A<sub>net</sub>; assimilated CO<sub>2</sub> μmol.m<sup>-2</sup>.s<sup>-1</sup>), stomatal conductance (G<sub>s</sub>; H<sub>2</sub>O mmol.m<sup>-2</sup>.s<sup>-1</sup>), and

transpiration rates (E;  $H_2O$  mmol.m<sup>-2</sup>.s<sup>-1</sup>). Instantaneous water use efficiency (WUE<sub>i</sub>) was calculated from  $A_{net}$  and E (WUE<sub>i</sub> = $A_{net}/E$ ).

### **Lignin Quantitation**

The second set of plants were harvested after 32-d, washed in NPW, and the second fully expanded leaves from the apical meristem across all the treatments (n=4) were severed and individually ground into a fine powder in liquid nitrogen using a set of mortar and pestle, rinsed with ethanol between samples. The ground leaf tissues were stored at -80°C for lignin quantitation, proteomic and metabolomic analyses.

Lignin was determined in the leaves using the acetyl bromide method. Priefly, 0.3 g ground tissues were freeze dried (FreeZone 6 L, -50°C; Labconco). Protein-free cell wall pellets obtained from the ground tissues were digested in 25% acetyl bromide and neutralized with 2 mol/L NaOH, and subsequently solubilized in freshly prepared 5 mol/L hydroxylamine-HCl solution. The samples were allowed to settle overnight, and the absorbance was measured at 280 nm.

## **Proteomic Analysis**

*LC-MS/MS analysis of peptides*. Proteins in the frozen ground leaves of each treatment group were extracted following Majumdar et al.<sup>25</sup> After trypsin digestion (1:20), the samples were desalted using 3M-Empore-C18 extraction disk-cartridge and analyzed using a Thermo Ultimate 3000 nano-liquid-chromatography system coupled to a Thermo Q-Exactive-plus Orbitrap mass spectrometer.<sup>26, 27</sup> The raw proteomics data have been deposited in the ProteomeXchange Consortium via the PRIDE partner repository with the dataset identifier PXD026456.<sup>28</sup> The detailed method for protein identification, quantification and statistical analysis is provided in SI Method S2. In summary, relative label-free quantification (LFQ) of the acquired data was performed using MaxQuant software (*v*.1.6.17.0) based on the intensity of peptides identified in a

full m/z scan. The MS/MS spectra were searched against the G. max UniProtKB database (85,051 entries; January 2021) using Andromeda search engine, and the peptide spectrum match and protein false discovery rate (FDR) was filtered at 1%. <sup>27, 29</sup> Protein abundance in the leaves was calculated based on spectral intensities (LFQ intensity) of the matched peptides normalized across all the treatments. Data Processing. Four separate analysis for feature detection and protein identification/ quantification was performed with different subsets (1) all treatment groups, (2) Control and CNW, (3) CNW and Kocide, and (4) Control and CuSO<sub>4</sub> to identify treatment specific proteins. Further processing of the quantitative data obtained on protein groups identified in soybean leaves across three independent biological replicates per treatment was performed using Perseus software (v.1.6.15.0), as described in SI Method S2.<sup>30</sup> The proteins were validated across the treatments and respective LFQ intensities were subjected to analysis of variance (ANOVA) controlled by  $p \le 0.05$ to identify the significant proteins, and clustered into groups by hierarchical clustering analysis based on Pearson's correlation. Functional annotation and Gene Ontology (GO) of the identified proteins was performed using UniprotKB and KEGG tools. 31, 32

## **Metabolomic Analysis**

228

229

230

231

232

233

234

235

236

237

238

239

240

241

242

243

244

245

246

247

248

249

250

For initial screening of the metabolites of interest, LC-MS/MS based untargeted and targeted metabolomic analyses were performed on the leaves from plants exposed to CNW-H, Kocide, CuSO<sub>4</sub>, and control, in triplicates, as described in SI Method S3. Briefly, finely ground tissues were extracted in the solvent mixture by vortex mixing for 90 min at  $4^{\circ}$ C. The extracted samples were centrifuged at  $16,000 \times g$  for 15 min at  $4^{\circ}$ C, and the supernatants were subjected to untargeted analysis of non-polar metabolites and targeted analysis of polar metabolites. The non-polar fraction of the supernatants were analyzed on a Waters<sup>TM</sup> Synapt G2-Si quadrupole time-of-

flight mass spectrometer coupled to an I-class UPLC system (SI Method S3).<sup>33</sup> The MS scan range was 50 to 1600 m/z with a 100 ms scan time and MS/MS was acquired in data-dependent fashion. Targeted analysis of 184 polar metabolites were performed on a Waters<sup>TM</sup> TO-XS triplequadrupole mass spectrometer coupled to an I-class UPLC system, and the MS was operated in selected reaction monitoring mode.<sup>34</sup> To delve deeper into metabolic pathways, targeted LC-MS/MS analysis of different groups of metabolites was performed in the leaves from plants exposed to CNW-L, CNW-M, CNW-H, Kocide, CuSO<sub>4</sub>, and control, each with four biological replicates. Frozen ground leaf tissues (~100 mg) were extracted in 1 ml of 80% methanol containing 2% formic acid, followed by vortex, sonication, and centrifugation at 20,000  $\times g$  at 4°C for 20 min at each step. The supernatants were used for the detection and quantification of 82 key metabolites including amino acids, antioxidants, fatty acids, organic acids/phenolics, nucleobase/side/tides, and sugar/ sugar alcohols, with independent methods for each metabolite group using an Agilent 1260 UHPLC binary pump coupled with an Agilent 6470 triple-quadrupole mass spectrometer, as previously described.<sup>27, 35,</sup> <sup>36</sup> The list of metabolites and the information on retention time, parent and product ions and linearity of the calibration curves are provided in Table S1. Data processing. A detailed description of the data processing has been provided in SI Method S3. For untargeted metabolomics data, the mass spectral data were processed using Progenesis Qi software (Nonlinear Dynamics).<sup>37-39</sup> An extension of the metabolomics standard initiative guidelines was used to assign annotation level confidence. 40, 41 Data acquired on Waters TM TQ-XS MS were processed using Skyline software. 42 The targeted data acquired on Agilent 6470 MS were processed using Agilent MassHunter software (v.B.06.00). Statistical analysis of the metabolites was performed using Metaboanalyst 5.0.<sup>43</sup>

251

252

253

254

255

256

257

258

259

260

261

262

263

264

265

266

267

268

269

270

271

272

### **Bioinformatics and Pathway Analysis**

The differentially accumulated proteins (DAPs) in the soybean exposed to CNWs and Kocide were used for protein-protein interaction (PPI) analysis using STRING database (https://string-db.org; v.11.0) with a high-confidence interaction score ( $\geq 0.7$ ) and pathway enrichment was performed using G. max database.<sup>44</sup> Metaboanalyst 5.0 was used for pathway enrichment using the metabolites of interest.<sup>43</sup> The common pathways from proteomic and metabolic analysis were merged to investigate the mechanism of interaction.

### **RESULT AND DISCUSSION**

### **Characterization of CNW and Kocide Suspensions**

The aqueous suspensions of copper hydroxide nanowires at three treatment levels (CNW-L, CNW-M, and CNW-H) and Kocide were characterized for particle size and surface charge at 0, 24, 48 and 96 h after sonication. The average hydrodynamic diameter of CNW-L, CNW-M, and CNW-H at 0 h was  $616 \pm 11$ ,  $604 \pm 60$ , and  $551 \pm 31$  nm, respectively (Figure 1A). Although a decreasing trend in hydrodynamic size of the aggregates was noted with increasing CNW concentration, it was statistically insignificant (p > 0.7). Kocide particles formed significantly (p = 0.006) larger aggregates ( $829 \pm 40$  nm), compared to CNWs. The  $\zeta$ -potentials of the CNW-L, CNW-M, CNW-H and Kocide particles were  $22.8 \pm 0.4$ ,  $20.8 \pm 0.2$ ,  $14.4 \pm 0.2$ , and  $-67.3 \pm 1.6$  mV respectively. (Figure 1B). In contrast to positively-charged CNWs, large stable aggregates and negative charge of Kocide particles in suspension is attributed to the organic moieties that bound Cu(OH)<sub>2</sub> nanosheets in the formulation.<sup>8, 45</sup> Sonication was determined as the preferred method for resuspension as vortex mixing was inefficient in resuspending CNWs in water when stored for 96 h (Figure S2). At high concentration, CNW aggregates rapidly within 24 h and vortex mixing is not enough to resuspend them. However, 15 min sonication successfully resuspended the CNW

in suspension at all concentrations. The organic binder in Kocide enables the particles to remain stable for at least 96 h in aqueous suspension, irrespective of the resuspension method.

### Plant growth, Copper Mobility and Nutrient Acquisition

297

298

299

300

301

302

303

304

305

306

307

308

309

310

311

312

313

314

315

316

317

318

319

Soybean plants did not show any overt symptoms of toxicity in response to CNW or Kocide (Table S2, Figure S3). Although there was an apparent increase in shoot length after 32- and 52-d exposure to CNW-H and 52-d exposure to Kocide, the increase was not statistically significant. However, acute exposure to Cu(II)-ions from CuSO<sub>4</sub> solutions showed discoloration of the exposed leaves, which suggests impairment of chlorophyll to function normally in the photosynthetic process. 46 The negative effect of direct exposure to Cu(II)-ions was reflected in the decreased shoot length of the plants, compared to other treatments. Copper accumulation was determined in soybean roots, aerial tissues exposed to Cu treatments (exposed shoot), and newly formed aerial tissues (unexposed shoot) (Figure 2A-D). Determination of Cu in shoot tissues without surface rinsing confirmed that CNW-M and Kocide-exposed shoots were sprayed with similar Cu levels (999  $\pm$  2 and 1084  $\pm$  63  $\mu$ g/g tissue) (Figure 2C). Compared to CNW-M exposure, CNW-L and CNW-H exposed shoots yielded around 5 times lower (241  $\pm$ 9  $\mu$ g/g tissue) and 5 times higher (5282 ± 195  $\mu$ g/g tissue) Cu levels in shoots, respectively, thereby validating the spraying process. To test Cu absorption by the leaves after 24h of exposure, shoots were surface rinsed to remove adhering Cu particles on the leaf surface. CNW-L and CNW-M treatments showed >95% retention of Cu in shoot tissues; however, CNW-H and Kocide treatments showed 42% and 27% retention, respectively. This suggests increased bioavailability and less wash-off of CNWs compared to Kocide treatment, hence better resource utilization. After 16-d exposure to CNW-L, CNW-M, CNW-H, Kocide and CuSO<sub>4</sub>, the exposed shoot tissues accumulated 78, 331, 948, 102, and 12.7 µg Cu/g tissue, respectively, and the unexposed tissues

accumulated 12, 29, 113, 18, and 9 µg Cu/g tissue, respectively (Figure 2A). Similarly, after 32-d exposure to similar Cu dose (1.2 mg/plant), CNW-M showed increased Cu accumulation in the unexposed tissues (32 µg/g) compared to Kocide treatment (10 µg/g) (Figure 2B). After 32-d of exposure, Cu content in the shoot tissues of CNW-M and CNW-H treated plants decreased compared to 16-d; however simultaneous increase in root Cu content in the 32-d treatments was observed with respect to 16-d (Figure 2D). The translocation factors were calculated as [Cu]<sub>unexposed</sub> shoot/[Cu]exposed shoot and [Cu]root/[Cu]exposed shoot. The aerial translocation factor after 16-d exposure was in the order of CuSO<sub>4</sub>> Kocide> CNW-L> CNW-H> CNW-M; however, after 32-d, CNW-L showed higher aerial translocation than Kocide (Table S3). Copper translocation to the roots was also highest in CuSO<sub>4</sub>, followed by CNW-L, Kocide, CNW-M, and CNW-H. Kocide and CuSO<sub>4</sub> treatments resulted in low Cu accumulation in shoots compared to CNW-M treatments after 16-d, which could be attributed to two factors: (1) lower Cu absorption by the leaf tissues (Figure 3C), and (2) higher rate of translocation to newer unexposed tissues and roots (Table S3) in Kocide and CuSO<sub>4</sub> treatments, which may also result in exudation via roots to avoid toxicity. This also suggests slow release and translocation of Cu from the applied CNWs compared to Kocide and ionic treatments, at similar or higher doses. Higher aerial translocation and limited translocation to roots of Cu from nanoscale Cu compounds have also been previously reported, demonstrating increased xylem transfer of Cu. 10, 17, 21, 47 Our study however suggests that CNW foliar exposure may not be the best choice if the application demands translocation to the roots.<sup>21</sup> Although CNW-L exposed shoots accumulated significantly less Cu than CNW-M and CNW-H, it accumulated significantly more Zn than other Cu treatments after 16-d exposure (Table S4). CuSO<sub>4</sub> exposure resulted in decreased Co accumulation compared to CNW-H and Kocide, and increased Fe levels than control treatments. However, in the roots from 16-d, CNW exposure

320

321

322

323

324

325

326

327

328

329

330

331

332

333

334

335

336

337

338

339

340

341

exhibited dose-dependent response on K, Co, Fe, and Mn accumulation. Roots from 16-d CNW-L exposure accumulated significantly higher levels of K, Co, and Mn, compared to CNW-M and CNW-H; whereas CNW-H roots accumulated high levels of Fe compared to all Cu treatments. The high Cu content in CNW-H shoots may activate redox-cycling between Fe and Cu, and chelation of the metal to ligands, metallochaperones, or storage proteins. This may also affect the photosynthetic electron transport, which is heavily dependent of Fe- and Cu-associated proteins in the chloroplast. Copper, Zn, Fe, and Mn are redox-active metals which participate as cofactors in Cu/Zn-SODs, Fe-SODs and Mn-SODs as the first line of defense against reactive oxygen species (ROS). The simultaneous dysregulation in Cu, Fe, Mn, and Zn levels in CNW-L indicate probable activation of SODs at low exposure doses. In 32-d exposed shoot tissues, the Cu treatments did not interfere with nutrient acquisition (Table S5). However, the roots from CuSO4 exposure showed depleted levels Co, Fe, Mn, and Zn. This could be a defense strategy by the CuSO4 treated plants to restrict micronutrient uptake in response to rapid Cu translocation to the unexposed tissues, thereby resulting in stunted aerial growth in these plants (Figure S3).

## **Lignification and Gas Exchange Activities**

Lignin is a complex and branched polymer of phenolic compounds, which is the final product of the phenylpropanoid pathway in plants and plays a crucial role in the defense response of plants. In the exposed leaves, only CNW-M treatment showed significantly high lignin accumulation (Figure S4). However, the unexposed fresh leaves from CNW-M, CNW-H, and Kocide treatments showed an increasing trend in lignin content, compared to control, but statistically significant only for Kocide treatment. The unexposed and exposed leaves from CNW-L treatment accumulated significantly less lignin than CNW-M, CNW-H, and Kocide treatments (p < 0.05). After 32-d exposure, the lignin content in the unexposed fresh leaves returned to normal

levels. Studies have suggested that Cu acts as a cofactor in enzymes such as laccase and peroxidase; hence, during the early growth stage, laccase could be responsible for lignin biosynthesis in Cu-treated tissues; and with prolonged incubation period, laccases and peroxidases may work cooperatively in lignin biosynthesis.<sup>48</sup> Compared to untreated control plants, net photosynthesis rate was significantly higher in plants exposed to Kocide and CuSO<sub>4</sub> after 12-d exposure; however, after longer exposure for 21-d, A<sub>net</sub> was significantly higher in all the treatments, except CNW-L and CNW-M (Figure 3A). The CuSO<sub>4</sub>, CNW-H, Kocide, and CNW-M treatments resulted in 21.3%, 20.3%, 16.6%, and 11.5% increase in A<sub>net</sub>, respectively. Similar increasing trend was observed in stomatal conductance rates in the plants after 21-d exposure to CNW-M, CNW-H, Kocide, and CuSO<sub>4</sub> (Figure 3B). The transpiration rates were however increased within 5-d exposure to all the treatments, but only significant for Kocide and CuSO<sub>4</sub>, compared to control (Figure 3D). With increasing period of exposure (12- and 21-d) the transpiration rates were consistently high for all the treatments, except CNW-L. Interestingly, the WUE<sub>i</sub> decreased in all the treatments, compared to control within 5-d exposure to all the treatments. However, it was restored to normal levels after 12-d in all Cu-treated plants (Figure 3D). As observed in the plants after 21-d exposure, high rates of A<sub>net</sub> may deplete concentrations of CO<sub>2</sub> in the chloroplast and increase mesophyll and stomatal conductance. The trend observed in the gas exchange rates could be attributed to Cu accumulation in the fresh tissues (Figure 2). Since foliar exposures to the Cu treatments were made on older mature leaves that were not used in gas-exchange measurements, the delayed response after 21-d of exposure may be explained by the low mobility of Cu in plant tissues, especially for CNW treatments (Figure 2). CNW-H exposure resulted in the highest Cu accumulation in the newly developed leaves, demonstrating enhancing effect on the photosynthetic process which was comparable to Kocide

366

367

368

369

370

371

372

373

374

375

376

377

378

379

380

381

382

383

384

385

386

387

exposure. In a previous study, Cu(II)-ion and nCuO exposure administered through soil application, negatively affected the gas exchange activities in bell pepper plants grown for 90 days;<sup>49</sup> however, our study demonstrate that foliar application of Cu improve the overall photosynthetic process in soybeans.

### Proteomic response in soybean plants exposed to CNW

389

390

391

392

393

394

395

396

397

398

399

400

401

402

403

404

405

406

407

408

409

410

411

To understand the underlying mechanisms of the physiological response to Cu treatments, proteomic analysis was performed on the leaf samples harvested after 32-d exposure. A total of 6,822 peptides corresponding to 1,645 protein groups were identified in the soybean leaves across all the treatments, including control, CNW-L, CNW-M, CNW-H, Kocide, and CuSO<sub>4</sub>. Proteins were validated by their presence in at least two replicates of at least one treatment and were considered as high-confidence proteins (Table S6). Of the protein groups identified across all the treatments, 19 were common among all Cu treatments, and absent in untreated control (Figure S5, Table S7). These proteins were predominant in mitochondrial and chloroplast thylakoid membrane, involved in chlorophyll-binding, metal-ion binding and ATP-binding and transmembrane transport, suggesting activation of Cu-associated regulatory networks. Some of these proteins were also involved in oxidoreductase activities including shikimate 3dehydrogenase (NADP+) activity, which plays critical role in aromatic amino acid biosynthesis (Phe, Tyr, and Trp) through shikimate pathway.<sup>50</sup> In addition, 18 proteins located in cytoplasm, mitochondria, chloroplast and peroxisomes were unique to CNW and CuSO<sub>4</sub> treatments, which were primarily associated with ATP- and metal ion-binding, and oxidoreductase activity in lignin biosynthetic process and fatty acid β-oxidation (Figure S5). Three unique proteins in CNW and Kocide treatments were associated with ATP-binding and hydrolases involved in proteolysis and amino-acid metabolism. Five proteins, viz. pectinesterase, isopentenyl-diposphate  $\delta$ -isomerase,

glycosyltransferase, and glutathione S-transferase, Leuk-A4-hydroC-domain-containing protein were exclusive to CNW treatments which were involved in cell wall modification, chlorophyll biosynthesis, flavonoid glycosylation, glutathione metabolism, and Zn-binding, respectively. Compared to control, all the CNW treatments accumulated 12 proteins which were located in mitochondrial proton-transporting ATP-synthase complex, chloroplast thylakoid membrane, nucleus, peroxisomes, and cytosol involved in ion transport, response to oxidative stress, NADP/NADH metabolism, nitrogen metabolic processes, flavonoid and carbohydrate metabolism, photosynthesis, catalytic activity (peroxidase, transferase, lyase, hydrolase), nucleobase-binding, vitamin-binding, and carbohydrate-binding.

Multi-scatter analysis was performed to examine the reproducibility of the quantification among the triplicates in each treatment groups. The average Pearson's correlation coefficient of the replicates within each treatment was  $\geq 0.95$ , suggesting a high degree of correlation (Figure S6). PLS-DA score plot of the identified proteins across all treatments shows that CNW-L and CNW-H treatments were separated from control, Kocide and CuSO<sub>4</sub> treatments along component 1 (19.7%) (Figure S7A). When the proteins identified in control and CNW treatments were processed separately, a clear separation of the CNW treatments and control is noted along component 1 (12.3%) (Figure S7B). One-way ANOVA identified 15 differentially accumulated proteins (DAPs) between all treatments at  $p \leq 0.05$  (Figure S8). However, separate analysis of proteins from CNW and control treatments was performed to identify CNW-specific protein abundance, which yielded 48 DAPs (Figure 4A, Table S8). Hierarchical clustering analysis grouped the DAPs into three distinct clusters based on abundance (Figure 4B, Table S9). Cluster-1 had 15 protein-groups that showed higher abundance in CNW-L treatment compared to control, CNW-M and CNW-H. Although CNW-L did not show overt physiological effect, the proteomics

results suggest activation of carbohydrate metabolism, lignin biosynthesis, and defense response in soybean plants, employing unique proteins that are not activated when Cu is present at higher abundance. Cluster 2 consisted of 7 protein-groups, that over-accumulated in all the CNW treatments, but most abundant in CNW-M treatment. It includes a cytosol protein, linoleate 9Slipoxygenase, that is involved in fatty acid biosynthesis, and a chloroplast protein, allene-oxide cyclase, which plays a key role in jasmonic acid biosynthesis. Thus, these set of proteins were involved in defense response to cope with high influx of Cu into the cells. Cluster 3 consisted of 26 protein-groups which were significantly down-accumulated in CNW-L leaves, out of which 15 were down-accumulated in all the CNW treatments. These proteins were primarily involved in translation, mitochondrial L-ornithine transmembrane transport, chlorophyll biosynthesis, oxidoreductase activities, and glutaminyl-peptide cyclotransferase activity. In the same cluster, 9 proteins were significantly over-accumulated in CNW-H and CNW-M treatments compared to control and CNW-L, of which 5 were present in chloroplast stroma/thylakoid and participated in ATP binding and ribulose-1,5-bisphosphate carboxylase-oxygenase (RuBisCo) activation. Other cytosol proteins were associated with metal-ion binding, fructose-bisphosphate aldolase activity and alpha-amylase activity involved in carbohydrate metabolism. Thus, the increase in A<sub>net</sub> in CNW-H and CNW-M treatments can be explained by the over-accumulation of proteins involved in photosystem I and II reactions and energy production, thereby leading to increase in shoot length. However, Kocide treatment modulated 41 proteins in the sobean leaves; 21 proteins were over-accumulated compared to control, which were involved in glycogen and starch biosynthesis, phosphatidylcholine activity, GTP binding, and structural constitution of ribosome for translation. The remaining 20 proteins showed decreased abundance, which were related to carbohydrate

435

436

437

438

439

440

441

442

443

444

445

446

447

448

449

450

451

452

453

454

455

metabolism, fatty acid  $\beta$ -oxidation, Fe-binding and hydrogen peroxide catabolic process, suggesting response to oxidative stress.

### Metabolomic response in soybean plants exposed to CNW

457

458

459

460

461

462

463

464

465

466

467

468

469

470

471

472

473

474

475

476

477

478

479

LC-MS/MS-based untargeted metabolomic analysis of the leaves across four treatment groups, including control, CNW-H, Kocide, and CuSO<sub>4</sub> resulted in the detection of 3361 semipolar to non-polar metabolites. As seen in the PLS-DA plot, Kocide was separated from control and CNW-H along component 1 at 27.3%, and the hierarchical clustering based on variable importance in projection (VIP) score illustrates the distinct metabolic features in the Kocide and CuSO<sub>4</sub> treatments (Figure S9A,B). However, there was no separation between control and CNW-H treatments and no significant features were noted. When the data analysis for metabolite concentrations in control and CNW-H was performed excluding the other Cu treatments, the separation was clear along component 1, but only two features were significant at FDR  $\leq 0.05$ . Combined targeted analysis of the polar metabolites identified 60 metabolites in the soybean leaves. The 2D-PLS-DA score plot suggests that the polar metabolites from Kocide were distinct from control (Figure S10A). Top fifteen important features were identified using VIP score ≥ 1, which predominantly included amino acids and nucleotides, or their derivatives (Figure S10B). The soybean metabolites modulated in response to Kocide treatments was comparable to previous studies. However, CNW-H treatment only showed abundance of cyclic guanosine monophosphate, compared to control. As distinct proteomic featured were observed at different CNW doses (Figure 4), a deeper approach was undertaken further using targeted metabolomics, by analyzing different groups of metabolites using independent LC-MS/MS methods. PLS-DA score plot suggests that a clear separation between CNW-L and other treatments (Figure 5, Figure S11), similar to the proteomic

analysis. Seventeen metabolites were differentially accumulated in the leaves of CNW-L treated plants compared to control (Figure 5), which includes five sugars (glucose, sucrose, galactose, fructose, and mannose) and eleven amino acids (Asn, Cit, Ser, Hse, Thr, Ala, Val, Pro, Ile, Leu, Gln). In CNW-M treated plants, Phe, Thr, Ile, Ala, Val and Pro were over-accumulated. However, most of the metabolite levels were lower in CNW-H leaves compared to control and other CNW treatments (Figure S10B, S12), which could be due to higher Cu concentration in the CNW-H shoots. Interestingly, all the Cu treatments including CNW-L, CNW-M, CNW-H, Kocide and CuSO<sub>4</sub> resulted in decrease in the concentration of salicylic acid. Salicylic acid is a phenolic compound which plays a crucial role in plants to alleviate stress due to heavy metals or other abiotic factors. 51. Compared to control, in Kocide and CuSO<sub>4</sub> treatments, linolenic acid levels were also lowered, which is involved in jasmonic acid biosynthesis. Jasmonic acid is another signaling molecule involved in plant stress response to biotic and abiotic factors.<sup>52</sup> The amino acid. Glu. which plays a central role in amino acid metabolism and glutathione cycle,<sup>53</sup> was significantly increased in Kocide and CuSO<sub>4</sub> treated plants; although the CNW treatments also showed an increasing trend, but they were not statistically significant (Figure S11).

## Biological pathways activated in response to CNW and Kocide

480

481

482

483

484

485

486

487

488

489

490

491

492

493

494

495

496

497

498

499

500

501

Mapping of the metabolites and proteins modulated by the CNW and Kocide treatments suggested that both treatments impacted aminoacyl-tRNA biosynthesis, amino acid metabolism, glyoxylate/dicarboxylate metabolism, nitrogen metabolism, phenylpropanoid biosynthesis, galactose metabolism, alkaloid biosynthesis, sulfur metabolism, sphingolipid metabolism, carbon fixation in photosynthetic process, starch/sucrose metabolism, glycolysis, fatty acid metabolism, and nucleotide metabolism (Table S10, 11).

The major biological processes that were affected by CNW treatment was photosynthesis and carbon fixation (Figure 6). At lower CNW concentration, the enzymes associated with chlorophyll biosynthesis, oxidoreductase activity and mitochondrial L-Orn transmembrane transport were less abundant; however, at higher concentration (CNW-M and CNW-H), these enzymes located in chloroplast and mitochondrial membrane were activated resulting in increased RuBisCo activity, ATP-binding and transmembrane transport. Plastocyanin is a Cu-containing photosynthetic enzyme that mediates transport of electron in thylakoids from stacked grana where photosystem II takes place, to unstacked regions that harbor photosystem I. 54 Hence, increased Cu availability improves the photosynthetic process in CNW treated plants, at higher concentration. This also corroborates with the elemental composition which shows increased Fe concentration in CNW-M and CNW-H shoots, which is also involved in the photosynthetic process. CNW-H treatment also yielded an increase in fructose-bisphosphate aldolase, which participates in glycolysis to convert fructose 1,6 bisphosphate to glyceraldehyde-3-phosphate. Alpha-amylase that catalyzes the hydrolysis of alpha-1,4-glucosidic bonds of glycogen, starch and related polysaccharides was also accumulated significantly more in the CNW-H-treated plants, suggesting increase in energy production (Table S10). The hexose levels were however lower in the leaves from CNW-H treatments, compared to control and other Cu treatments, which could be explained by utilization of these metabolites for energy production, resulting in increased shoot length of the CNW-H treated plants (Figure S3). Increase in the accumulation of the hexose sugars (sucrose, glucose, fructose, mannose, galactose) in the leaves from CNW-L and CNW-M treated plants signify increase in the photosynthetic activity, however, the gas exchange activities did not show any significant effects at the lower dose. This also corroborates the proteomic findings, where sucrose synthase, alpha-galactosidase,

502

503

504

505

506

507

508

509

510

511

512

513

514

515

516

517

518

519

520

521

522

523

and glucan endo-1,3-beta-glucosidase were over-accumulated in CNW-L and CNW-M demonstrating activation of sugar metabolism. NADH dehydrogenase (ubiquinone) 4Fe-4S protein complex showed enhanced levels in CNW-L treated plants. This protein participates in electron transfer from NADH to the respiratory chain.<sup>55</sup> Another enzyme, 6-phosphogluconate dehydrogenase, was also over-accumulated in CNW-L and CNW-M leaves. 6-phosphogluconate dehydrogenase catalyzes the decarboxylating reduction of 6-phosphogluconate into ribulose 5phosphate in the presence of nicotinamide adenine dinucleotide phosphate (NADP) in pentosephosphate pathway, which is a parallel pathway to glycolysis. CNW-M also activated fatty acid biosynthesis as noted by the increased levels of lipoxygenase and allene-oxide cyclase; however, the gas exchange activities did not show any significant effects at the lower dose. In terms of stress response, γ-glutaminyl-peptide cyclotransferase level was enhanced in CNW-M and CNW-H leaves, whereas it was significantly less abundant in the lower exposure dose. This enzyme converts Gln and N-terminal glutamyl residues in peptides to 5-oxoproline and 5oxoproline residues. This was also reflected in the metabolomic analysis, where Gln was significantly decreased in all the treatments with respect to control, except CNW-L. CNW-M and CNW-H resulted in increased levels of cinnamyl-alcohol dehydrogenase, which is directly involved in lignin biosynthesis via phenylpropanoid pathway. However, salicylic acid, an early product of the shikimate pathway was decreased in all Cu treatments, suggesting an active stress response by the soybean plants against Cu treatments. The activation of the phenylpropanoid pathways in the CNW and Kocide treatments corroborates the lignin accumulation results which showed high levels after 16-d exposure in all the treatments, except CNW-L (Figure S4). In CNW-L, increased levels of ferulic acid formed from the phenylpropanoid pathway was responsible for alleviating oxidative stress.

525

526

527

528

529

530

531

532

533

534

535

536

537

538

539

540

541

542

543

544

545

546

Although most stress response pathways were activated by CNW at the highest concentrations, Kocide treatment induced more stress response pathways and modulated amino acid synthesis involved in various metabolic processes. Only Kocide treatment resulted in increased accumulation of antioxidant compounds including Glu, α-tocopherol and amino acid precursors for the phenylpropanoid pathway (Phe, Tvr, and Trp). In addition, Met was exclusively overaccumulated in Kocide exposed plants, resulting in the activation of Cys-Met metabolism. These S-containing amino-acids are precursors to various antioxidant metabolites such as glutathione, phytochelatins, S-adenosylmethionine, ethylene, and polyamines.<sup>56</sup> In addition, two proteins, Sadenosylmethionine synthase and methionine synthase, were also over-accumulated in Kocidetreated plants. The activation of stress response in the plants upon exposure to Kocide plants corroborates previous studies reporting the impact on oxidative stress and amino acid metabolism in corn, lettuce, cucumber and spinach plants. 11, 12, 18, 57 Thus, from integration of proteomic and metabolomic fingerprints we conclude that CNW at low concentration activates the sugar and fatty acid metabolism, but only activates the pathways involved in photosynthesis and energy metabolism at higher concentrations (Figure 6). Although Kocide also activates the sugar metabolism and energy production, it activates a greater number of oxidative stress pathways, which could be due to rapid availability of Cu during early exposure period in contrast to CNW treatments, where Cu translocation is slower. It was apparent from the Cu accumulation studies that CNW exposure resulted in slow release of Cu to the aerial and root tissues, compared to Kocide and CuSO<sub>4</sub> treatments. This also results in differential response in the metabolic processes of the soybean plants. This study highlights the use and integration of proteomics and multi-platform metabolomics to elucidate the molecular mechanisms leading to physiological and metabolic alterations in plants

548

549

550

551

552

553

554

555

556

557

558

559

560

561

562

563

564

565

566

567

568

569

in response to engineered nanomaterials. This study for the first time revealed the proteins and metabolites in soybean plants associated with the response to CNW in comparison to Kocide by utilizing omic approaches. Integration of discovery proteomics with metabolomics identified photosynthesis, carbohydrate metabolism, amino acid metabolism, phenylpropanoid biosynthesis, fatty acid metabolism as the major metabolic pathways that were affected by CNW and Kocide exposure. A holistic understanding of the underlying molecular mechanisms and the factors influencing the uptake and biological response can result in safer application of copper-based nano-pesticides in the future.

### Acknowledgements

This material is based upon work supported by the National Science Foundation under Grant No. 1901515. We thank Dr. Yu Chen and the Molecular Instrumentation Center, UCLA Department of Chemistry & Biochemistry for desalting and running the proteomic samples on LC-MS/MS. We thank the UC Riverside Metabolomics Core for providing instrumentation for metabolomics analysis. Any opinions, findings, and conclusions or recommendations expressed in this material are those of the author(s) and do not necessarily reflect the views of the National Science Foundation.

### ASSOCIATED CONTENT

**Supporting Information.** Proteomic and metabolomic analysis; foliar spray exposure set-up schematic; growth and biomass of soybean plants after foliar exposure to control, CNW-L, CNW-M, CNW-H, Kocide, and CuSO<sub>4</sub>; gas exchange parameters in soybean plants after 21 days of foliar exposure; size and  $\zeta$ -potential of suspensions after 0, 24, 48, and 96 h; Identified and differentially accumulated proteins in the leaves of soybean plants; Identified and differentially accumulated

- 593 metabolites in the leaves of soybean plants; This material is available free of charge at
- 594 http://pubs.acs.org.

#### References

- 1. Kah, M.; Tufenkji, N.; White, J. C., Nano-enabled strategies to enhance crop nutrition and protection. *Nature Nanotechnology* **2019**, *14*, (6), 532-540.
- 598 2. Iavicoli, I.; Leso, V.; Beezhold, D. H.; Shvedova, A. A., Nanotechnology in agriculture: Opportunities, toxicological implications, and occupational risks. *Toxicology and applied pharmacology* **2017**, *329*, 96-111.
- 3. Majumdar, S.; Keller, A. A., Omics to address the opportunities and challenges of nanotechnology in agriculture. *Critical Reviews in Environmental Science and Technology* **2020**, 1-42, https://doi.org/10.1080/10643389.2020.1785264.
- 4. Marschner, H., Preface to Second Edition. In *Marschner's Mineral Nutrition of Higher Plants* (Third Edition), Marschner, P., Ed. Academic Press: San Diego, 2012; p ix.
- 5. Ravet, K.; Pilon, M., Copper and iron homeostasis in plants: the challenges of oxidative stress.
   Antioxid Redox Signal 2013, 19, (9), 919-932.
- 608 6. Yruela, I., Copper in plants. *Brazilian Journal of Plant Physiology* **2005**, *17*, 145-156.
- Reregistration Eligibility Decision (RED) for Coppers. In U.S. Environmental Protection
   Agency, O. o. P., Pesticides and Toxic Substances, Office of Pesticide Programs., Ed. U.S.
   Government Printing Office: Washington, DC, 2009.
- 8. Keller, A. A.; Adeleye, A. S.; Conway, J. R.; Garner, K. L.; Zhao, L.; Cherr, G. N.; Hong, J.;
  Gardea-Torresdey, J. L.; Godwin, H. A.; Hanna, S.; Ji, Z.; Kaweeteerawat, C.; Lin, S.; Lenihan,
- H. S.; Miller, R. J.; Nel, A. E.; Peralta-Videa, J. R.; Walker, S. L.; Taylor, A. A.; Torres-Duarte, C.; Zink, J. I.; Zuverza-Mena, N., Comparative environmental fate and toxicity of copper
- 615 C.; Zink, J. I.; Zuverza-Mena, N., Comparative environmental fate and toxicity of copper nanomaterials. *NanoImpact* **2017**, *7*, 28-40.
- Tamez, C.; Hernandez-Molina, M.; Hernandez-Viezcas, J. A.; Gardea-Torresdey, J. L.,
   Uptake, transport, and effects of nano-copper exposure in zucchini (Cucurbita pepo). Science of The Total Environment 2019, 665, 100-106.
- 10. Hong, J.; Rico, C. M.; Zhao, L.; Adeleye, A. S.; Keller, A. A.; Peralta-Videa, J. R.; Gardea-Torresdey, J. L., Toxic effects of copper-based nanoparticles or compounds to lettuce (Lactuca sativa) and alfalfa (Medicago sativa). *Environmental Science: Processes & Impacts* 2015, 17, (1), 177-185.
- 11. Zhao, L.; Ortiz, C.; Adeleye, A. S.; Hu, Q.; Zhou, H.; Huang, Y.; Keller, A. A., Metabolomics to Detect Response of Lettuce (Lactuca sativa) to Cu(OH)2 Nanopesticides: Oxidative Stress Response and Detoxification Mechanisms. *Environmental Science & Technology* 2016, 50, (17), 9697-9707.
- 12. Zhao, L.; Huang, Y.; Keller, A. A., Comparative Metabolic Response between Cucumber (Cucumis sativus) and Corn (Zea mays) to a Cu(OH)2 Nanopesticide. *J Agric Food Chem* 2018, 66, (26), 6628-6636.
- 13. Zhao, L.; Huang, Y.; Hannah-Bick, C.; Fulton, A. N.; Keller, A. A., Application of metabolomics to assess the impact of Cu(OH)2 nanopesticide on the nutritional value of lettuce (Lactuca sativa): Enhanced Cu intake and reduced antioxidants. *NanoImpact* **2016**, *3-4*, 58-66.
- 14. Zhao, L.; Huang, Y.; Adeleye, A. S.; Keller, A. A., Metabolomics Reveals Cu(OH)2
   Nanopesticide-Activated Anti-oxidative Pathways and Decreased Beneficial Antioxidants in
   Spinach Leaves. *Environmental Science & Technology* 2017, 51, (17), 10184-10194.
- 15. Zhao, L.; Hu, Q.; Huang, Y.; Fulton, A. N.; Hannah-Bick, C.; Adeleye, A. S.; Keller, A. A., Activation of antioxidant and detoxification gene expression in cucumber plants exposed to a Cu(OH)2 nanopesticide. *Environmental Science: Nano* **2017**, *4*, (8), 1750-1760.

- 16. Valdes, C.; Cota-Ruiz, K.; Flores, K.; Ye, Y.; Hernandez-Viezcas, J. A.; Gardea-Torresdey, J. L., Antioxidant and defense genetic expressions in corn at early-developmental stage are differentially modulated by copper form exposure (nano, bulk, ionic): Nutrient and physiological effects. *Ecotoxicology and Environmental Safety* **2020**, *206*, 111197.
- 17. Zhao, L.; Huang, Y.; Zhou, H.; Adeleye, A. S.; Wang, H.; Ortiz, C.; Mazer, S. J.; Keller, A. A., GC-TOF-MS based metabolomics and ICP-MS based metallomics of cucumber (Cucumis sativus) fruits reveal alteration of metabolites profile and biological pathway disruption induced by nano copper. *Environmental Science: Nano* **2016**, *3*, (5), 1114-1123.
- 18. Zhao, L.; Huang, Y.; Paglia, K.; Vaniya, A.; Wancewicz, B.; Keller, A. A., Metabolomics Reveals the Molecular Mechanisms of Copper Induced Cucumber Leaf (Cucumis sativus) Senescence. *Environmental Science & Technology* **2018**, *52*, (12), 7092-7100.
- 19. Ma, C.; Borgatta, J.; Hudson, B. G.; Tamijani, A. A.; De La Torre-Roche, R.; Zuverza-Mena,
   N.; Shen, Y.; Elmer, W.; Xing, B.; Mason, S. E.; Hamers, R. J.; White, J. C., Advanced material
   modulation of nutritional and phytohormone status alleviates damage from soybean sudden
   death syndrome. *Nature Nanotechnology* 2020, *15*, (12), 1033-1042.
- 20. Elmer, W.; De La Torre-Roche, R.; Pagano, L.; Majumdar, S.; Zuverza-Mena, N.; Dimkpa,
   C.; Gardea-Torresdey, J.; White, J. C., Effect of Metalloid and Metal Oxide Nanoparticles on
   Fusarium Wilt of Watermelon. *Plant Disease* 2018, 102, (7), 1394-1401.
- 21. Borgatta, J.; Ma, C.; Hudson-Smith, N.; Elmer, W.; Plaza Pérez, C. D.; De La Torre-Roche,
   R.; Zuverza-Mena, N.; Haynes, C. L.; White, J. C.; Hamers, R. J., Copper Based Nanomaterials
   Suppress Root Fungal Disease in Watermelon (Citrullus lanatus): Role of Particle
   Morphology, Composition and Dissolution Behavior. ACS Sustainable Chemistry &
   Engineering 2018, 6, (11), 14847-14856.
- 22. Cota-Ruiz, K.; Ye, Y.; Valdes, C.; Deng, C.; Wang, Y.; Hernández-Viezcas, J. A.; Duarte-Gardea, M.; Gardea-Torresdey, J. L., Copper nanowires as nanofertilizers for alfalfa plants:
   Understanding nano-bio systems interactions from microbial genomics, plant molecular responses and spectroscopic studies. *Science of The Total Environment* 2020, 742, 140572.
- 23. Kim, E.; Hwang, S.; Lee, I., SoyNet: a database of co-functional networks for soybean Glycine max. *Nucleic acids research* **2017**, *45*, (D1), D1082-D1089.
- 24. Moreira-Vilar, F. C.; Siqueira-Soares, R. d. C.; Finger-Teixeira, A.; Oliveira, D. M. d.; Ferro,
   A. P.; da Rocha, G. J.; Ferrarese, M. d. L. L.; dos Santos, W. D.; Ferrarese-Filho, O., The
   Acetyl Bromide Method Is Faster, Simpler and Presents Best Recovery of Lignin in Different
   Herbaceous Tissues than Klason and Thioglycolic Acid Methods. *PloS one* 2014, 9, (10),
   e110000.
- 25. Majumdar, S.; Almeida, I. C.; Arigi, E. A.; Choi, H.; VerBerkmoes, N. C.; Trujillo-Reyes, J.;
   Flores-Margez, J. P.; White, J. C.; Peralta-Videa, J. R.; Gardea-Torresdey, J. L., Environmental
   Effects of Nanoceria on Seed Production of Common Bean (Phaseolus vulgaris): A Proteomic
   Analysis. *Environmental Science & Technology* 2015, 49, (22), 13283-13293.
- 26. Kaiser, P.; Wohlschlegel, J., Identification of Ubiquitination Sites and Determination of
   Ubiquitin-Chain Architectures by Mass Spectrometry. In *Methods in Enzymology*, Academic
   Press: 2005; Vol. 399, pp 266-277.
- 27. Majumdar, S.; Pagano, L.; Wohlschlegel, J. A.; Villani, M.; Zappettini, A.; White, J. C.; Keller,
   A. A., Proteomic, gene and metabolite characterization reveal the uptake and toxicity
   mechanisms of cadmium sulfide quantum dots in soybean plants. *Environmental Science:* Nano 2019, 6, (10), 3010-3026.

- 28. Perez-Riverol, Y.; Csordas, A.; Bai, J.; Bernal-Llinares, M.; Hewapathirana, S.; Kundu, D. J.;
  Inuganti, A.; Griss, J.; Mayer, G.; Eisenacher, M.; Pérez, E.; Uszkoreit, J.; Pfeuffer, J.;
  Sachsenberg, T.; Yilmaz, S.; Tiwary, S.; Cox, J.; Audain, E.; Walzer, M.; Jarnuczak, A. F.;
  Ternent, T.; Brazma, A.; Vizcaíno, J. A., The PRIDE database and related tools and resources
  in 2019: improving support for quantification data. *Nucleic acids research* 2019, 47, (D1),
- 29. Cox, J.; Mann, M., MaxQuant enables high peptide identification rates, individualized p.p.b. range mass accuracies and proteome-wide protein quantification. *Nature Biotechnology* 2008,
   26, 1367.

705

D442-D450.

- 30. Tyanova, S.; Temu, T.; Sinitcyn, P.; Carlson, A.; Hein, M. Y.; Geiger, T.; Mann, M.; Cox, J.,
   The Perseus computational platform for comprehensive analysis of (prote)omics data. *Nature Methods* 2016, *13*, 731.
- 31. The UniProt, C., UniProt: a worldwide hub of protein knowledge. *Nucleic Acids Research* **2018**, *47*, (D1), D506-D515.
- 32. Morishima, K.; Tanabe, M.; Furumichi, M.; Kanehisa, M.; Sato, Y., New approach for understanding genome variations in KEGG. *Nucleic Acids Research* **2018**, *47*, (D1), D590-D595.
- 33. Rothman, J. A.; Leger, L.; Kirkwood, J. S.; McFrederick, Q. S., Cadmium and selenate exposure affects the honey bee microbiome and metabolome, and bee-associated bacteria show potential for bioaccumulation. *Appl Environ Microbiol* 2019, 85(21):e01411-19.
- 34. Vliet, S. M. F.; Dasgupta, S.; Sparks, N. R. L.; Kirkwood, J. S.; Vollaro, A.; Hur, M.; Zur Nieden, N. I.; Volz, D. C., Maternal-to-zygotic transition as a potential target for niclosamide during early embryogenesis. *Toxicol Appl Pharmacol* 2019, 380, 114699.
- 35. Huang, Y.; Adeleye, A. S.; Zhao, L.; Minakova, A. S.; Anumol, T.; Keller, A. A., Antioxidant response of cucumber (Cucumis sativus) exposed to nano copper pesticide: Quantitative determination via LC-MS/MS. *Food Chemistry* 2019, 270, 47-52.
- 36. Huang, Y.; Li, W.; Minakova, A. S.; Anumol, T.; Keller, A. A., Quantitative analysis of changes in amino acids levels for cucumber (Cucumis sativus) exposed to nano copper.
   NanoImpact 2018, 12, 9-17.
- 37. Dunn, W. B.; Broadhurst, D.; Begley, P.; Zelena, E.; Francis-McIntyre, S.; Anderson, N.;
  Brown, M.; Knowles, J. D.; Halsall, A.; Haselden, J. N.; Nicholls, A. W.; Wilson, I. D.; Kell,
  D. B.; Goodacre, R.; Consortium, H. S. M. H., Procedures for large-scale metabolic profiling
  of serum and plasma using gas chromatography and liquid chromatography coupled to mass
  spectrometry. *Nat Protoc* 2011, 6, (7), 1060-83.
- 38. Barupal, D. K.; Fan, S.; Wancewicz, B.; Cajka, T.; Sa, M.; Showalter, M. R.; Baillie, R.;
  Tenenbaum, J. D.; Louie, G.; Kaddurah-Daouk, R.; Fiehn, O.; Initiative, A. s. D. N.;
  Consortium, A. s. D. M., Generation and quality control of lipidomics data for the alzheimer's disease neuroimaging initiative cohort. *Sci Data* 2018, 5, 180263.
- 39. Broeckling, C. D.; Afsar, F. A.; Neumann, S.; Ben-Hur, A.; Prenni, J. E., RAMClust: a novel feature clustering method enables spectral-matching-based annotation for metabolomics data. *Anal Chem* **2014**, *86*, (14), 6812-7.
- 40. Sumner, L. W.; Amberg, A.; Barrett, D.; Beale, M. H.; Beger, R.; Daykin, C. A.; Fan, T. W.;
  Fiehn, O.; Goodacre, R.; Griffin, J. L.; Hankemeier, T.; Hardy, N.; Harnly, J.; Higashi, R.;
  Kopka, J.; Lane, A. N.; Lindon, J. C.; Marriott, P.; Nicholls, A. W.; Reily, M. D.; Thaden, J.
- 730 J.; Viant, M. R., Proposed minimum reporting standards for chemical analysis Chemical

- Analysis Working Group (CAWG) Metabolomics Standards Initiative (MSI). *Metabolomics* **2007**, *3*, (3), 211-221.
- 41. Schymanski, E. L.; Jeon, J.; Gulde, R.; Fenner, K.; Ruff, M.; Singer, H. P.; Hollender, J., Identifying small molecules via high resolution mass spectrometry: communicating confidence. *Environ Sci Technol* **2014**, *48*, (4), 2097-8.
- 42. MacLean, B.; Tomazela, D. M.; Shulman, N.; Chambers, M.; Finney, G. L.; Frewen, B.; Kern,
   R.; Tabb, D. L.; Liebler, D. C.; MacCoss, M. J., Skyline: an open source document editor for creating and analyzing targeted proteomics experiments. *Bioinformatics* 2010, 26, (7), 966-8.
- 43. Chong, J.; Soufan, O.; Li, C.; Caraus, I.; Li, S.; Bourque, G.; Wishart, D. S.; Xia, J.,
   MetaboAnalyst 4.0: towards more transparent and integrative metabolomics analysis. *Nucleic Acids Research* 2018, 46, (W1), W486-W494.
- 44. Szklarczyk, D.; Morris, J. H.; Cook, H.; Kuhn, M.; Wyder, S.; Simonovic, M.; Santos, A.;
   Doncheva, N. T.; Roth, A.; Bork, P.; Jensen, L. J.; von Mering, C., The STRING database in
   2017: quality-controlled protein-protein association networks, made broadly accessible.
   Nucleic acids research 2017, 45, (D1), D362-D368.
- 45. Adeleye, A. S.; Conway, J. R.; Perez, T.; Rutten, P.; Keller, A. A., Influence of Extracellular
   Polymeric Substances on the Long-Term Fate, Dissolution, and Speciation of Copper-Based
   Nanoparticles. *Environmental Science & Technology* 2014, 48, (21), 12561-12568.
- 46. Amberger, A.; Gutser, R.; Wunsch, A., Iron chlorosis induced by high copper and manganese supply. *Journal of Plant Nutrition* 1982, 5, (4-7), 715-720.
- 47. Keller, A. A.; Huang, Y.; Nelson, J., Detection of nanoparticles in edible plant tissues exposed to nano-copper using single-particle ICP-MS. *J Nanopart Res* **2018**, *20*, (4), 101.
- 48. Lin, C.-C.; Chen, L.-M.; Liu, Z.-H., Rapid effect of copper on lignin biosynthesis in soybean roots. *Plant Science* **2005**, *168*, (3), 855-861.
- 49. Rawat, S.; Pullagurala, V. L. R.; Hernandez-Molina, M.; Sun, Y.; Niu, G.; Hernandez-Viezcas,
   J. A.; Peralta-Videa, J. R.; Gardea-Torresdey, J. L., Impacts of copper oxide nanoparticles on
   bell pepper (Capsicum annum L.) plants: a full life cycle study. *Environmental Science: Nano* 2018, 5, (1), 83-95.
- 50. Ye, S.; Von Delft, F.; Brooun, A.; Knuth, M. W.; Swanson, R. V.; McRee, D. E., The crystal structure of shikimate dehydrogenase (AroE) reveals a unique NADPH binding mode. *J Bacteriol* 2003, 185, (14), 4144-4151.
- 51. Janda, T.; Gondor, O. K.; Yordanova, R.; Szalai, G.; Pál, M., Salicylic acid and photosynthesis:
   signalling and effects. *Acta Physiologiae Plantarum* 2014, 36, (10), 2537-2546.
- Wang, J.; Song, L.; Gong, X.; Xu, J.; Li, M., Functions of Jasmonic Acid in Plant Regulation
   and Response to Abiotic Stress. *International journal of molecular sciences* 2020, 21, (4),
   1446.
- 53. Forde, B. G.; Lea, P. J., Glutamate in plants: metabolism, regulation, and signalling. *Journal of Experimental Botany* **2007**, *58*, (9), 2339-2358.
- 54. Höhner, R.; Pribil, M.; Herbstová, M.; Lopez, L. S.; Kunz, H.-H.; Li, M.; Wood, M.; Svoboda,
   V.; Puthiyaveetil, S.; Leister, D.; Kirchhoff, H., Plastocyanin is the long-range electron carrier
   between photosystem II and photosystem I in plants. *Proceedings of the National Academy of Sciences* 2020, *117*, (26), 15354.
- 55. Wydro, M. M.; Sharma, P.; Foster, J. M.; Bych, K.; Meyer, E. H.; Balk, J., The evolutionarily
   conserved iron-sulfur protein INDH is required for complex I assembly and mitochondrial
   translation in *Arabidopsis*. *The Plant cell* 2013, 25, (10), 4014-4027.

- 56. Nikiforova, V.; Kempa, S.; Zeh, M.; Maimann, S.; Kreft, O.; Casazza, A. P.; Riedel, K.;
   Tauberger, E.; Hoefgen, R.; Hesse, H., Engineering of cysteine and methionine biosynthesis in potato. *Amino Acids* 2002, 22, (3), 259-278.
- 57. Zhao, L.; Huang, Y.; Hu, J.; Zhou, H.; Adeleye, A. S.; Keller, A. A., 1H NMR and GC-MS
   Based Metabolomics Reveal Defense and Detoxification Mechanism of Cucumber Plant under
   Nano-Cu Stress. *Environmental Science & Technology* 2016, 50, (4), 2000-2010.
- 58. Kosová, K.; Vítámvás, P.; Urban, M. O.; Prášil, I. T.; Renaut, J., Plant Abiotic Stress
   Proteomics: The Major Factors Determining Alterations in Cellular Proteome. 2018, 9, (122)
   , doi: 10.3389/fpls.2018.00122.

# 788 Figures

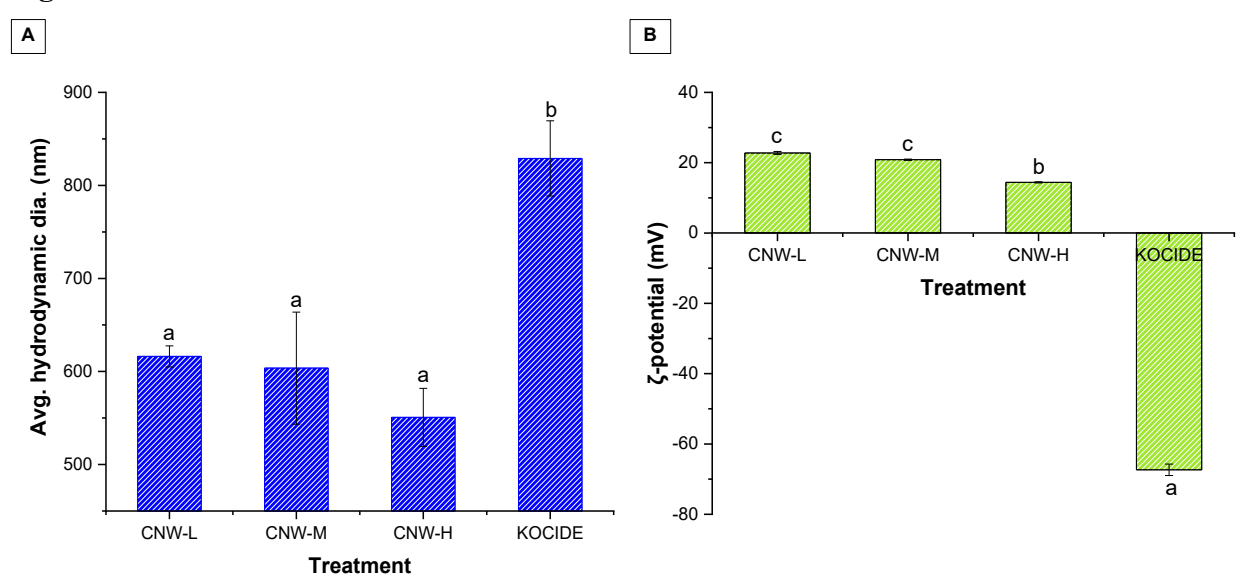


Figure 1. Characteristics of CNWs (CNW-L, CNW-M, CNW-H) and Kocide in aqueous suspension (A) Average hydrodynamic diameter (nm), (B)  $\zeta$ -potential (mV). Values are expressed as Mean  $\pm$  SE (n=4). Bars with different letters represent significant differences between the treatments, as determined by one-way ANOVA and Tukey's multiple comparison test ( $p \le 0.05$ ).

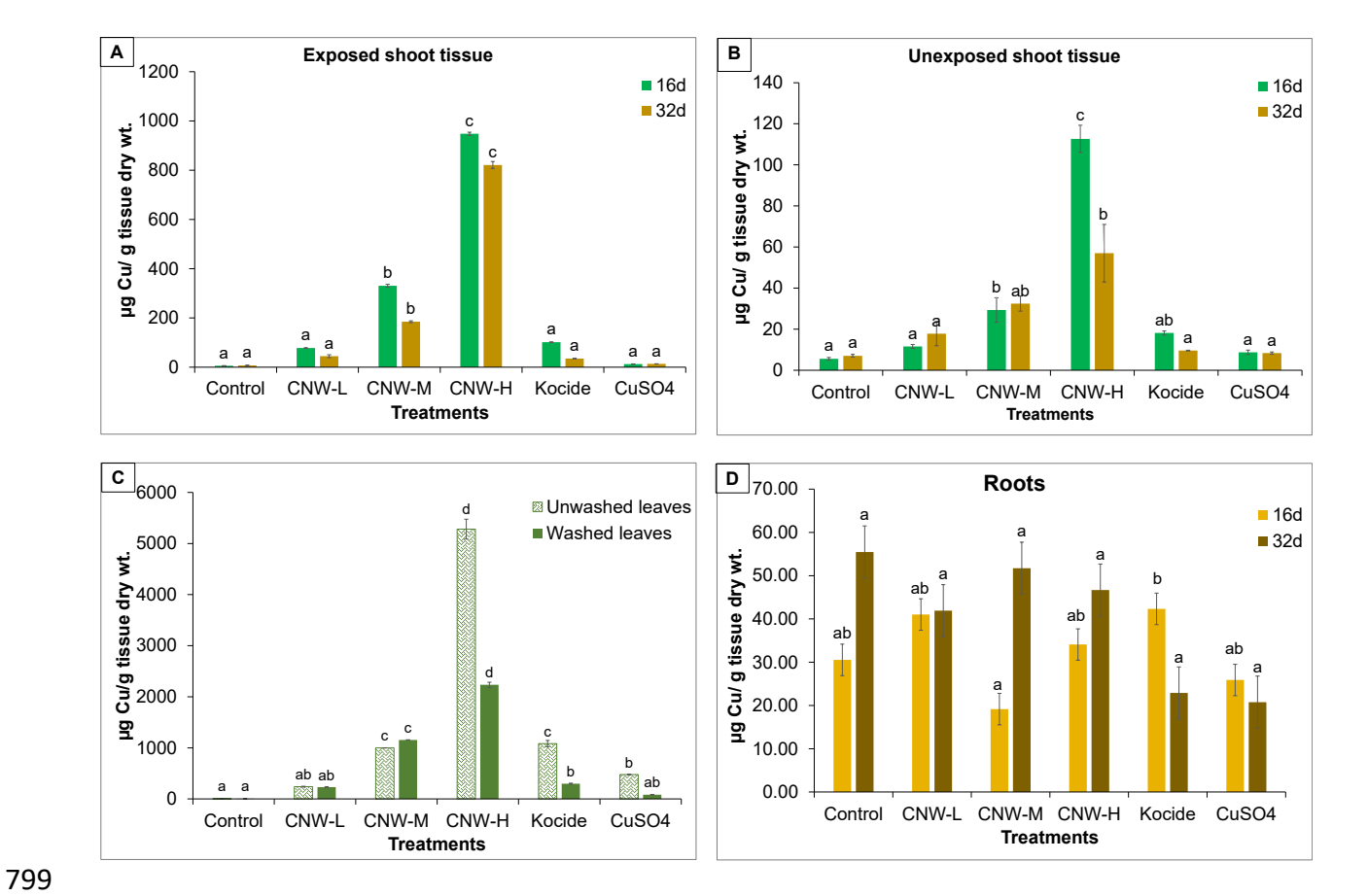


Figure 2. Copper concentration ( $\mu$ g Cu/g tissue dry weight) in plant tissues after foliar exposure to control, CNW-L, CNW-M, CNW-H, Kocide and CuSO<sub>4</sub> treatments (A) Exposed shoot tissues after 16- and 32-d; (B) Unexposed shoot tissues after 16- and 32-d; (C) Unwashed and washed exposed leaves after 1 d; (D) Roots after 16- and 32-d. Values are expressed as Mean  $\pm$  SE (n = 4). Bars with different letters represent significant differences between the treatments, as determined by one-way ANOVA and Tukey's multiple comparison test ( $p \le 0.05$ )

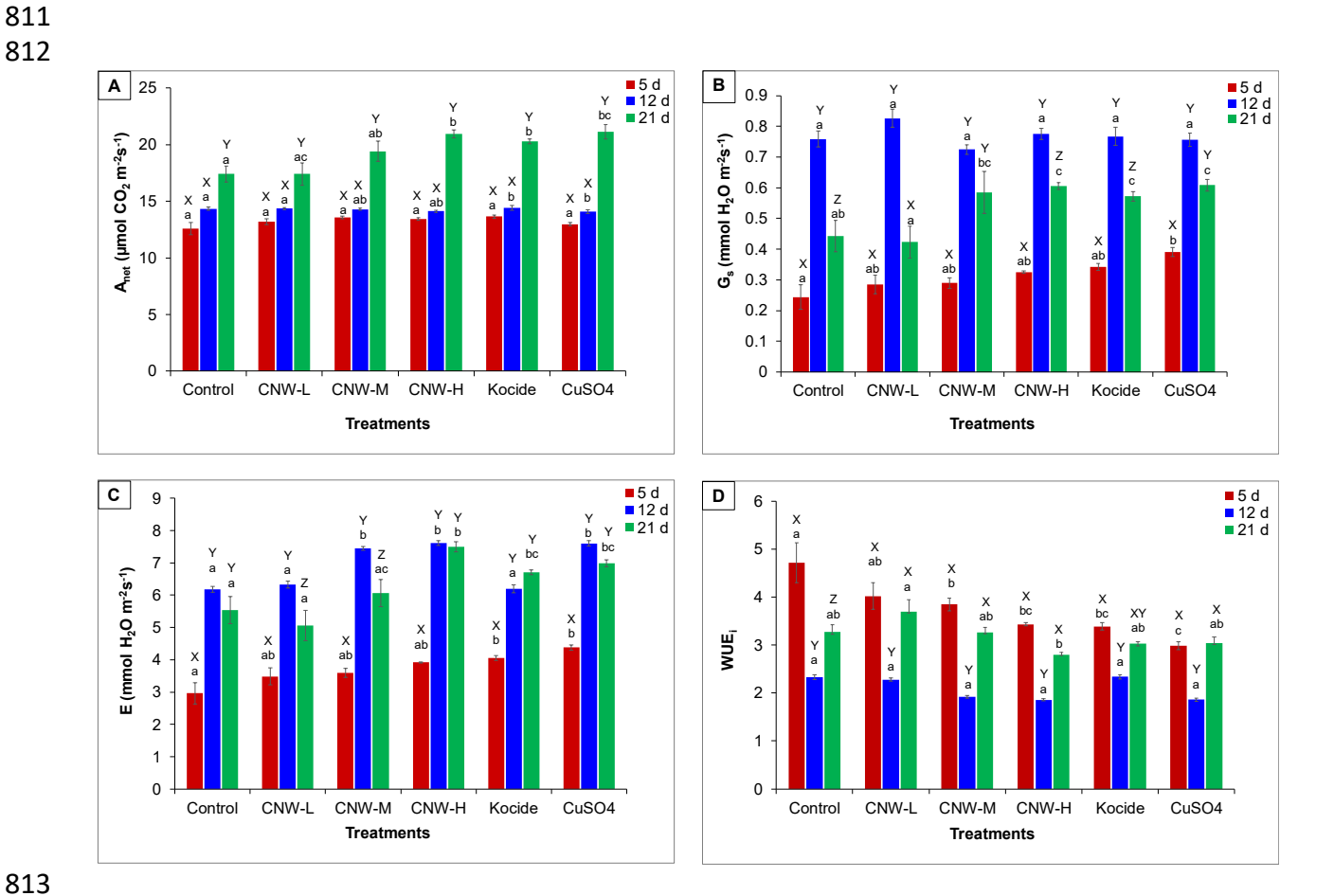


Figure 3. Gas exchange activities in soybean plants. (A) Net photosynthesis rate,  $A_{net}$  (µmol  $CO_2$   $m^{-2}$   $s^{-1}$ ) (B) Stomatal conductance rate,  $G_s$  (mmol  $H_2O$   $m^{-2}$   $s^{-1}$ ), (C) Transpiration rate, E (mmol  $H_2O$   $m^{-2}$   $s^{-1}$ ), (D) Water use efficiency, WUE<sub>i</sub> ( $A_{net}/E$ ) in the most recent fully expanded leaf after 5-, 12-, and 21-d foliar exposure to control, CNW-L, CNW-M, CNW-H, Kocide and CuSO<sub>4</sub> treatments. Values are expressed as Mean  $\pm$  SE (n=4). Bars with different letters represent significant difference between the treatments (a, b, c) and between days of exposure within a treatment (X, Y, Z), as determined by one-way ANOVA and Tukey's multiple comparison test ( $p \le 0.05$ ).

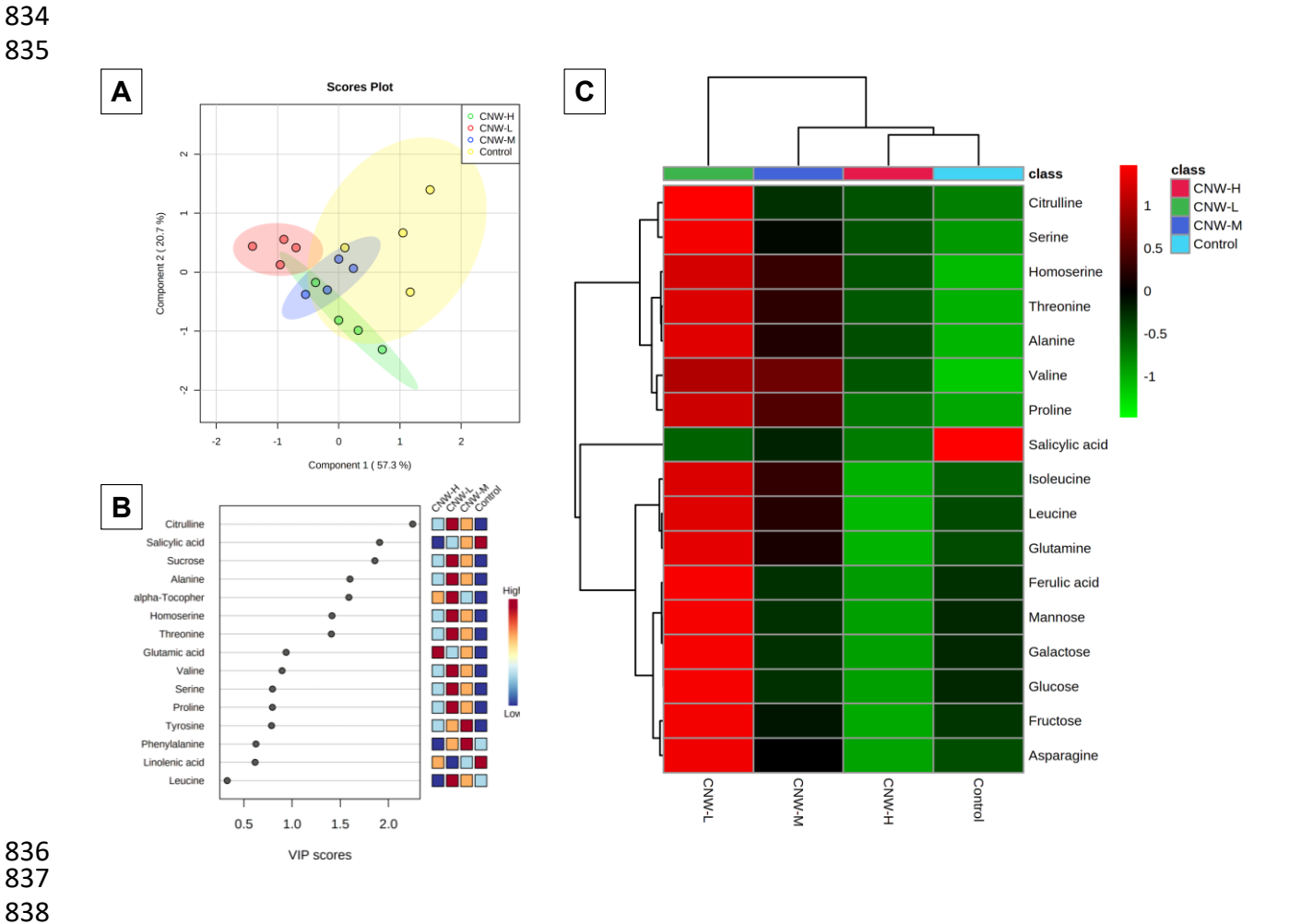


Figure 4. Targeted metabolomic analysis in the leaves of plants exposed to control, CNW-L, CNW-M, and CNW-H treatments. (A) PLS-DA score plot of metabolites identified (B) Important features identified by PLS-DA, the colored boxes indicate the relative concentrations of the corresponding metabolite in each group. (C) Hierarchical clustering of the ANOVA significant metabolites (FDR  $\leq 0.05$ ), the color bar shows the increase (red) and decrease (green) in the abundance of the metabolites.

854

855 856

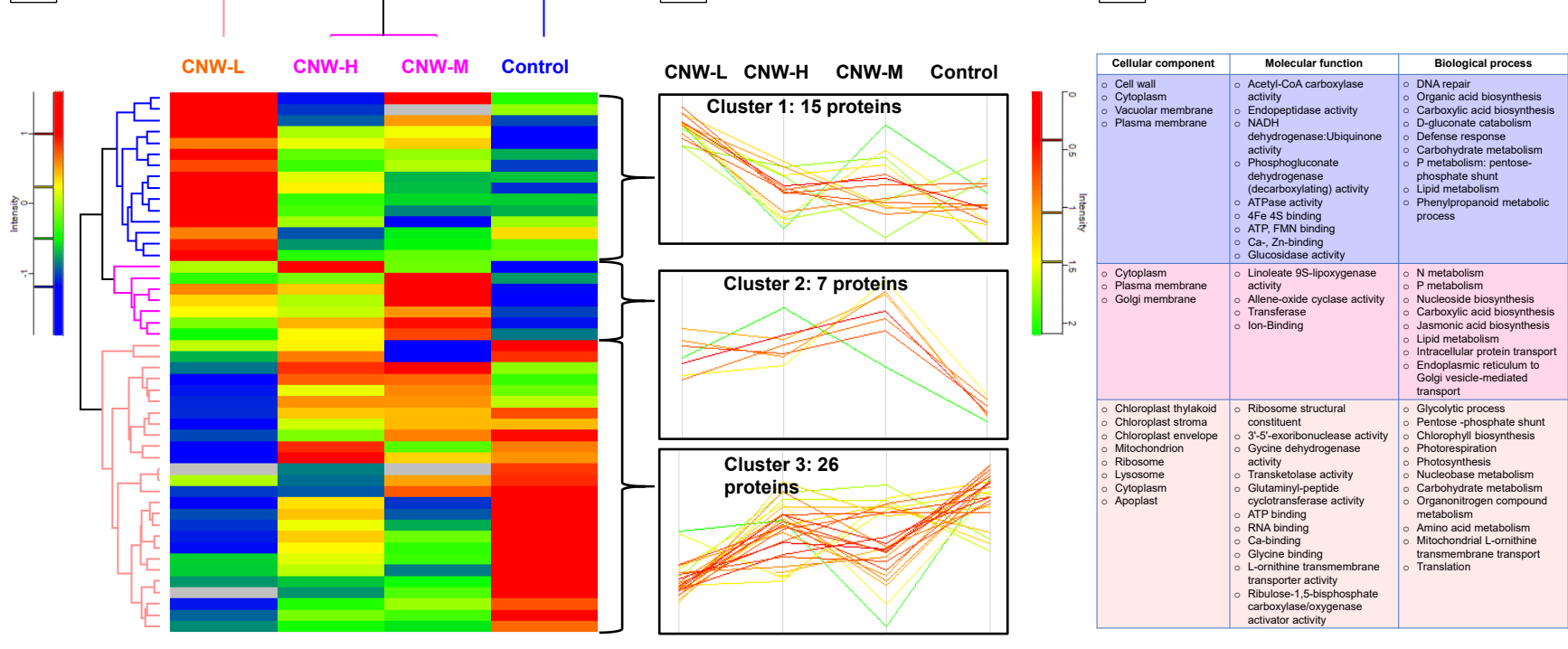


Figure 5. Hierarchical clustering analysis of ANOVA significant leaf proteins after 32-d foliar exposure to control, CNW-L, CNW-M, and CNW-H treatments. (A) Heat map demonstrating the clusters with the abundance scale shown in the legend; (B) Abundance pattern of the differentially accumulated proteins in three clusters; (C) Gene ontology of the three clusters

Figure 6. Schematic diagram of metabolic pathways in soybean plants activated in response to CNW treatments. Affected pathways and metabolites have been highlighted in red.

